Neoplasma 2023; 70(2): 260–271

doi:10.4149/neo_2023_221126N1140

The inhibition of Aurora A kinase regulates phospholipid remodeling by upregulating LPCAT1 in glioblastoma

Ya-Zhou MIAO[1,2,3,#], Jing WANG[1,#], Shu-Yu HAO[1,2], Yu-Xuan DENG[2], Zhe ZHANG[2], Ze-Ping JIN[2], Da-Yuan LIU[2,4], Shao-Dong ZHANG[1], Hong WAN[1], Nan JI[2,5,6,*], Jie FENG[1,*]

[1]Beijing Neurosurgical Institute, Capital Medical University, Beijing, China; [2]Department of Neurosurgery, Beijing Tiantan Hospital, Capital Medical University, Beijing, China; [3]Department of Neurosurgery, The First Affiliated Hospital of Zhengzhou University, Zhengzhou, Henan, China; [4]Department of Neurosurgery, The Second Affiliated Hospital of Hainan Medical University, Haikou, Hainan, China; [5]Beijing Advanced Innovation Center for Big Data-Based Precision Medicine School of Engineering Medicine, Beijing University, Beijing, China; [6]China National Clinical Research Center for Neurological Diseases, Beijing, China

**Correspondence: jinan@mail.ccmu.edu.cn, fengjie111@ccmu.edu.cn*
[#]Contributed equally to this work.

Received November 26, 2022 / Accepted April 18, 2023

Metabolic reprogramming is a common feature of glioblastoma (GBM) progression and metastasis. Altered lipid metabolism is one of the most prominent metabolic alterations in cancer. Understanding the links between phospholipid remodeling and GBM tumorigenesis may help develop new anticancer strategies and improve treatments to overcome drug resistance. We used metabolomic and transcriptomic analyses to systematically investigate metabolic and molecular changes in low-grade glioma (LGG) and GBM. We then re-established the reprogrammed metabolic flux and membrane lipid composition in GBM based on metabolomic and transcriptomic analyses. By inhibiting Aurora A kinase via RNA interference (RNAi) and inhibitor treatment, we investigated the effect of Aurora A kinase on phospholipid reprogramming LPCAT1 enzyme expression and GBM cell proliferation *in vitro* and *in vivo*. We found that GBM displayed aberrant glycerophospholipid and glycerolipid metabolism compared with LGG. Metabolic profiling indicated that fatty acid synthesis and uptake for phospholipid synthesis were significantly increased in GBM compared to LGG. The unsaturated phosphatidylcholine (PC) and phosphatidylethanolamine (PE) levels were significantly decreased in GBM compared to LGG. The expression level of LPCAT1, which is required for the synthesis of saturated PC and PE, was upregulated in GBM, and the expression of LPCAT4, which is required for the synthesis of unsaturated PC and PE, was downregulated in GBM. Notably, the inhibition of Aurora A kinase by shRNA knockdown and treatment with Aurora A kinase inhibitors such as Alisertib, AMG900, or AT9283 upregulated LPCAT1 mRNA and protein expression *in vitro*. *In vivo*, the inhibition of Aurora A kinase with Alisertib increased LPCAT1 protein expression. Phospholipid remodeling and a reduction in unsaturated membrane lipid components were found in GBM. Aurora A kinase inhibition increased LPCAT1 expression and suppressed GBM cell proliferation. The combination of Aurora kinase inhibition with LPCAT1 inhibition may exert promising synergistic effects on GBM.

Key words: metabolomics; phospholipid remodeling; glioblastoma; AURKA inhibitor; LPCAT1

Metabolic reprogramming is a common feature of cancer progression and metastasis. Cancer cells rewire metabolism to sustain both their growth and to adapt to harsh microenvironments. In addition to the well-known 'Warburg effect', that is, switching from oxidative phosphorylation to aerobic glycolysis, altered lipid metabolism is one the most prevalent metabolic alterations in cancer. Metabolic reprogramming confers metabolic dependency, which can be exploited for the therapeutic targeting of cancers [1]. Glioblastoma (GBM) is the most common primary malignant brain tumor and is almost always fatal in adults. There is an urgent need to develop effective therapeutic strategies for GBM.

Phospholipids are not only major constituents of biological membranes but also substrates for the generation of bioactive molecules involved in signal transduction, such as eicosanoids, lysophosphatidylcholine (LPC), lysophosphatidic acid (LPA), and diacylglycerol (DAG) [2–4]. Phospholipids in biological membranes are glycerophospholipids, which consist of two fatty acyl chains linked to a glycerol

backbone together with a hydrophilic headgroup. Among glycerophospholipids, phosphatidylcholine (PC) is the most abundant biological in cell membranes, accounting for 40–50% of all membrane phospholipids [4].

Fatty acids (FAs) are critical for the biophysical properties of the membrane, they are affected endogenously by fatty acid synthesis and exogenously by the dietary consumption of fatty acids [5]. Furthermore, the fatty acid composition of membrane phospholipids is regulated by various lysophospholipid acyltransferases (LPLATs) through a remodeling process – a pathway referred to as the Lands cycle [4, 6–8]. Due to the substrate specificity of enzymes, saturated fatty acyl chains such as palmitic acid (16:0) and stearic acid (18:0) are preferably linked to the glycerol backbone at the sn-1 position and polyunsaturated fatty acids (PUFAs) such as arachidonic acid (AA; 20:4), eicosapentaenoic acid (EPA; 20:5), and docosahexaenoic acid (DHA; 22:6) are linked at the sn-2 position [4, 8, 9].

Lysophosphatidylcholine acyltransferase 1 (LPCAT1) is a major PC-remodeling enzyme that catalyzes the conversion of LPCs into PCs in the remodeling PC pathway. Studies using genetic models have demonstrated that lysophosphatidylcholine acyltransferases (LPCATs) play important roles in lipid metabolism and homeostasis by regulating the abundance of different PC species in multiple cells and tissue types [4]. Consistent with LPCAT1 enzyme activity, the levels of saturated phospholipids are increased in these tumors [10]. Membrane lipid saturation plays an important role in the protection of cancer cells from oxidative stress-induced cell death [10, 11].

Currently, Aurora A kinase inhibitors are being tested in many clinical trials for the treatment of multiple cancer types. Aurora A, a serine/threonine kinase involved in cell cycle progression, has been mainly studied in the context of cell division and tumorigenesis. It is frequently overexpressed in various cancer types, and upregulated Aurora A expression has been widely proven to be associated with drug resistance and poor prognoses. In our previous study, it has been demonstrated that Aurora A kinase inhibitor Alisertib could activate epidermal growth factor receptor (EGFR) signaling in GBM (unpublished data). However, other studies indicated that activated EGFR signaling alters the phospholipid composition of GBM through increasing LPCAT1 expression [12]. Whether Aurora A kinase control the behaviors of cancer cells by affecting LPCAT1 expression and membrane lipid saturation has not been studied to date. Understanding how Aurora A expressed in synchrony with metabolic changes may have important therapeutic implications.

In this study, we identified lipid metabolism changes in GBM by integrating untargeted metabolomic data and ribose nucleic acid (RNA) expression profiling data and thus determined the effect of Aurora A kinase inhibitor treatment on phospholipid reprogramming enzyme LPCAT1 expression and GBM cell proliferation *in vitro* and *in vivo*.

Patients and methods

Human specimen acquisition. GBM (WHO IV, n=13) and LGG, WHO II, n=13 surgical specimens were obtained for untargeted metabolomic analysis. GBM (WHO IV, n=23) and LGG (WHO II, n=17) surgical specimens were obtained for RNA sequencing analysis. All the samples were obtained from Beijing Tiantan Hospital between June 2014 and September 2019. The study was approved by the Research Ethics Committee of Beijing Tiantan Hospital (KY2014-021-02), and informed consent was obtained from all the participating patients. The study was performed in compliance with the principles expressed in the Declaration of Helsinki.

Untargeted metabolomics. Tissues (100 mg) were individually grounded in liquid nitrogen, and the homogenate was resuspended in prechilled 80% methanol and 0.1% formic acid by extensive vortexing. The samples were incubated on ice for 5 min and then centrifuged at 15,000×g and 4°C for 20 min. Some of the supernatants were diluted to a final concentration containing 53% methanol in liquid chromatography-mass spectrometry (LC-MS) grade water. The samples were subsequently transferred to a fresh Eppendorf (EP) tube and then centrifuged at 15,000×g and 4°C for 20 min. Finally, the supernatant was injected into a liquid chromatography-tandem mass spectrometry (LC-MS/MS) system for analysis. To perform quality control, an equal volume of each experimental sample was mixed, and they were used as QC samples. The blank sample contained only 53% methanol aqueous solution, and the pretreatment process was the same for both the quality control and experimental samples.

Ultrahigh-performance (UHP) LC-MS/MS analyses were performed using a Vanquish UHPLC system (Thermo Fisher, Germany) coupled with an Orbitrap Q Exactive TMHF-X mass spectrometer (Thermo Fisher, Germany) by the Novogene Co., Ltd. (Beijing, China). Samples were injected into a Hypersil Gold column (100 × 2.1 mm, 1.9 μm) using a 17 min linear gradient at a flow rate of 0.2 ml/min. The eluents in positive polarity mode were 0.1% FA in water (eluent A) and methanol (eluent B). The eluents in negative polarity mode were 5 mM ammonium acetate, pH 9.0 (eluent A) and methanol (eluent B). The solvent gradient was set as follows: 2% eluent B for 1.5 min; 2–100% eluent B for 12.0 min; eluent 100% B for 14.0 min; 100–2% eluent B for 14.1 min; 2% eluent B for 17 min. The mass spectrometer was operated in positive/negative polarity mode with a spray voltage of 3.2 kV, capillary temperature of 320°C, a sheath gas flow rate of 40 arb, and an aux gas flow rate of 10 arb.

RNA sequencing. RNA was isolated from tumors with TRIzol reagent. After the quality of the RNA was verified, an Epicenter Ribo-Zero rRNA removal kit (Epicenter) was used to remove ribosomal RNA (rRNA). Subsequently, sequencing libraries were generated using rRNA-depleted RNA with a NEBNext Ultra Directional RNA Library Prep Kit for Illumina (NEB) following the manufacturer's recommen-

dations. Finally, Illumina HiSeq2000 was used to sequence the libraries, and transcripts with an adjusted $p<0.05$ were considered to be differentially expressed.

Cell culture and AURKA knockdown. The LN18, LN229, U87, and M059K human glioma cell lines were purchased from the American Type Culture Collection (ATCC) (Manassas, VA, USA); TJ905 and U373 human glioma cell lines were purchased from Procell Life Science & Technology Co., Ltd. (Wuhan, China). All the cells were cultured in Dulbecco's modified Eagle medium (DMEM) supplemented with 10% fetal bovine serum (Gibco, MA, USA) and 1% penicillin-streptomycin at 37°C with 5% CO_2. The cell lines used in this study tested negative for mycoplasma, as determined with a TransDetect PCR mycoplasma detection kit (TransGen, Beijing, China).

Reverse transcription-quantitative polymerase chain reaction (RT-qPCR). In this study, the mRNA expression levels of AURKA were evaluated in the LN18, LN229, U87, M059K, TJ905, and U373 glioma cell lines. Furthermore, RT-qPCR was performed to evaluate the knockdown efficiency of AURKA-shRNA and the mRNA expression levels of LPCAT1 after AURKA expression knockdown in the LN18 cell line. LPCAT1 expression levels were evaluated in the LN18 glioma cell lines after treatment with Aurora A kinase inhibitor Alisertib (5 μM, cat. no. S1133, Selleck Chemicals), AT9283 (75 nM, cat. no. S1134, Selleck Chemicals) and AMG900 (150 nM, cat. no. S2719, Selleck Chemicals) for 72 h. The details of the experiment are as follows: total RNA was isolated from the glioma cell lines using QIAzol lysis reagent (Qiagen Sciences, MD, USA). The cDNA was synthesized with a high-capacity cDNA reverse transcription kit (Applied Biosystems, CA, USA) and subsequently analyzed with QuantStudio 5 (Applied Biosystems, CA, USA). The amplification program was as follows: initial denaturation at 95°C for 30 s, followed by 40 cycles at 95°C for 15 s and 60°C for 60 s. The expression of each gene was calculated relative to the expression of the internal reference gene, GAPDH, using the $2^{-\Delta\Delta Ct}$ method. The primer sequences are shown in Supplementary Table S1.

Western blot analysis. In this study, western blotting was performed to evaluate Aurora A kinase expression levels in glioma cell lines and the knockdown efficiency of AURKA-shRNA. Additionally, the expression of LPCAT1 in LN18 cells treated with or without the Aurora A kinase inhibitor and AURKA-shRNA was detected by western blot assay. The details of the experiment are as follows: the cells were harvested with 0.05% trypsin, washed with cold PBS, and lysed with ice-cold nondenaturing lysis buffer supplemented with protease and phosphatase inhibitors. Then proteins were separated on 12% SDS polyacrylamide gels and transferred onto polyvinylidene fluoride (PVDF) membranes (Millipore, Billerica, CA, USA). After blocking the nonspecific binding sites with 5% skim milk in TBST buffer, the membranes were incubated with primary antibodies at 4°C overnight. Then the membranes were incubated with secondary horseradish peroxidase (HRP)-conjugated goat anti-rabbit or anti-mouse antibodies for 1 h at room temperature, and the specific protein bands were visualized using an enhanced chemiluminescence reagent. The antibodies used in this study were as follows: anti-AURKA (Cell Signaling Technology, #14475), anti-LPCAT1 (Abcam, ab214034), anti-GAPDH (Abcam, ab9485), and anti-β-Actin (Abcam, ab8227).

Cell viability assay. Cells were seeded in 96-well plates at a density of 5×10^3 cells/well and then incubated with dimethyl sulfoxide (DMSO, the control), AMG900 (cat. no. S2719, Selleck Chemicals), AT9283 (cat. no. S1134, Selleck Chemicals), or Alisertib (cat. no. S1133, Selleck Chemicals) for 72 h. After incubation, cell viability was assayed by Cell Counting Kit-8 (CCK-8) (Dojindo, Kumamoto, Japan), specifically, 10 μl of CCK-8 reagent was added to 100 μl of culture medium. Cells were incubated for 4 hours at 37°C until the culture turned orange. The absorbance of the CCK-8 reagent was measured with a microplate reader (BioTek, VT, USA) at 450 nm. Three replicates were established for each drug.

Animal study. GL261 glioma cells were directly purchased from ATCC and cultured in DMEM (Gibco, MA, USA) with 10% FBS (Gibco, MA, USA) and 1% penicillin-streptomycin (Gibco, MA, USA). GL261 is a malignant glioma cell line that is syngeneic to C57BL/6 mice. GL261 was tagged with luciferase by lentiviral infection (GL261-luc) and administered to female C57BL/6 mice at six weeks of age via intracranial injection using a stereotactic apparatus at a concentration of 2×10^5 GL261 cells in 5 μl PBS (HyClone, UT, USA). Fourteen days after GL261-luc cells were injected, the tumor-bearing mice were randomly divided into two groups: the control group and the Alisertib treatment group. The mice in the control group did not receive any treatment, and the mice in the Alisertib treatment group received 2 mg/kg Alisertib (MedChemExpress, NJ, USA) every day (oral, p.o.). After the surgery, the C57BL/6 mice were imaged weekly by an In Vivo Imaging System (IVIS, PerkinElmer, CA, USA) 10 min after 150 mg/kg D-luciferin (PerkinElmer, 122799) was intraperitoneally injected. The mice were euthanized when they exhibited neurological signs including hydrocephalus and hemiparesis. All animal protocols were approved by the Animal Welfare Ethics Committee of Beijing Neurosurgical Institute (No. 202104004).

Immunohistochemistry (IHC) staining. IHC staining was performed as follows. Briefly, slides were deparaffinized and rehydrated, and antigen retrieval was performed using EDTA Antigen Retrieval Solution. Then, the slides were treated with 0.3% H_2O_2 for 15 min to inhibit endogenous peroxidase activity and incubated with LPCAT1 polyclonal antibody (16112-1-AP, 1:500, ProteinTech) overnight at 4°C. The slides were washed carefully with PBS and incubated with the secondary antibody. DAB Peroxidase Substrate Kit (ZLI-9017, ZSGB-BIO) was used for the detection of LPCAT1 staining. The IHC staining score of LPCAT1 was quantified by two independent experienced pathologists. IHC scoring criterion was established by combining the positive propor-

tion of the stained tumor cells (1 for 0–25%, 2 for 26–50%, 3 for 51–75%, and 4 for >75%) and the staining intensity (0 for no staining, 1 for light yellow, 2 for yellowish brown, and 3 for brown). The final IHC scores were obtained using the following formula: final immunohistochemistry score (0–12) = values of intensity (0–3) × values of percentage counts (0–4).

Statistical and bioinformatics analysis. GraphPad Prism 8.0 (GraphPad Software, Inc., San Diego, CA, USA) and R (version 4.0.4, http://www.r-project.org) were used for statistical analysis and visualization in this study. All the quantitative data were presented as the mean ± SD on the basis of at least three samples. Differences between the two groups were evaluated by a two-tailed unpaired t-test, and differences between the three groups were evaluated by one-way ANOVA. A p-value <0.05 was considered to indicate a significant difference. MetaboAnalyst 5.0 was employed for untargeted metabolomics data analysis and integrative analysis of RNA sequencing data (https://www.metaboanalyst.ca/).

Results

Metabolic and molecular changes between LGG and GBM. All 26 subjects with LGG or GBM were tested for common metabolic and molecular changes. All samples were subjected to metabolomic analysis. Significant differences in metabolite levels between LGG and GBM samples were observed. A total of 1,003 metabolites were identified, and 225 of these metabolites were differentially expressed between the two groups (the criteria for differential expression were p-value <0.05, with a fold change >2 or <0.5). Specifically, in the GBM samples compared to the LGG samples, the expression levels of 141 metabolites were upregulated, and those of 84 were downregulated. The heatmaps show two-dimensional hierarchical clustering and indicate that the analyzed metabolites were clearly segregated in the samples of two groups, and their levels were consistent with the clinical diagnosis of patients (Figures 1A–1D). Addition-

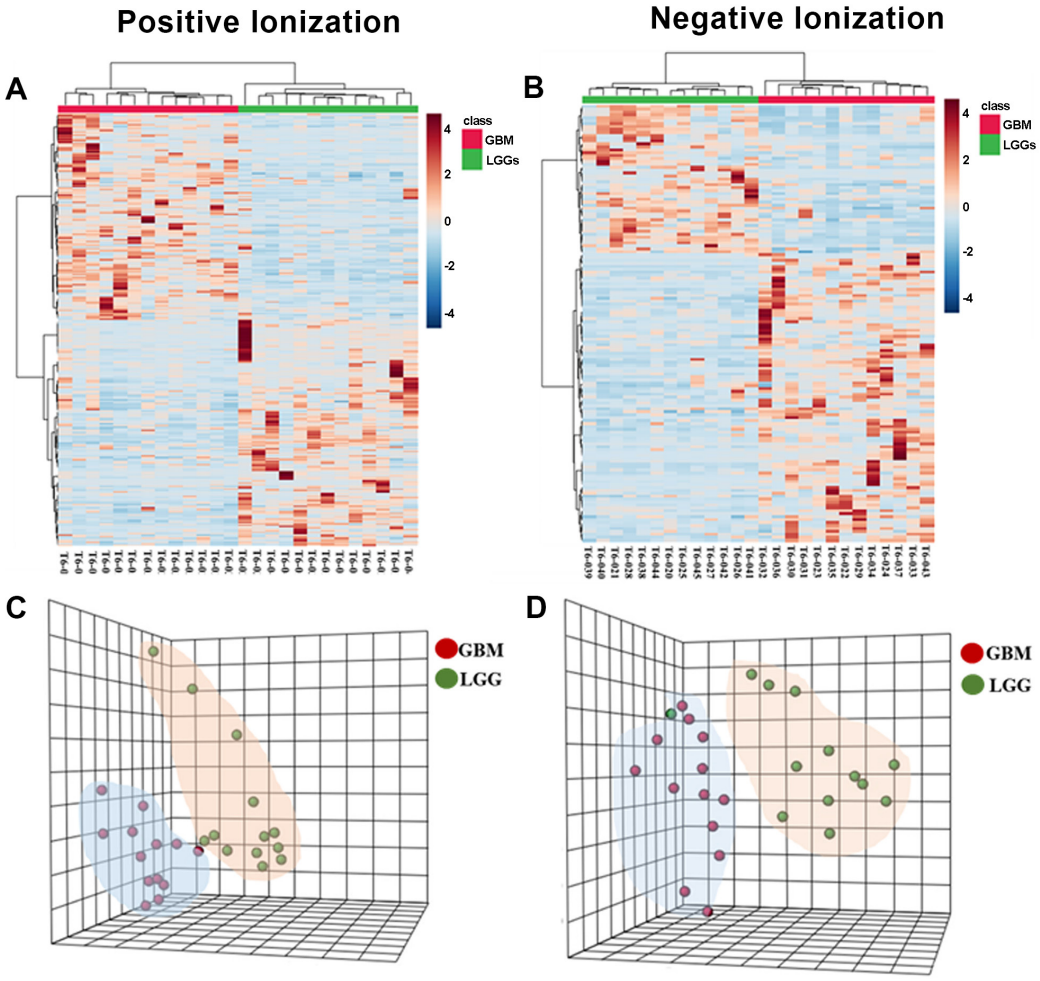

Figure 1. The difference in metabolite levels between GBM and LGG. The heatmaps and partial least squares discriminant analysis (PLS-DA) illustrated that the analyzed metabolites clearly segregated the samples into two groups. A, B) are two-dimensional clustering heatmaps. The horizontal axis represents each sample and the vertical axis represents each metabolite. A, C) display metabolites from the positive ionization model and B, D) display the metabolites from the negative ionization model.

ally, partial least squares discriminant analysis (PLS-DA) was also performed to determine that the GBM and LGG groups were truly different, and the metabolites between the GBM and LGG groups indicated the differences between these groups.

Joint pathway analysis of metabolites and genes and the comparison between LGG and GBM samples. Joint pathway analysis was performed on the basis of enrichment and topology analyses. The enrichment analysis led to the identification of genes and metabolites that were significantly enriched in a particular pathway ($p<0.05$; Figure 2A and Supplementary Table S2), and the results indicated that the metabolites were enriched in glycerophospholipid metabolism, glycolipid metabolism, linoleic acid metabolism, glycolysis or gluconeogenesis, alpha-linolenic acid metabolism, mucin-type O-glycan biosynthesis, lysine degradation, glutathione metabolism, nitrogen metabolism, purine metabolism, and beta-alanine metabolism. The topology analysis led to the identification of genes or metabolites that likely played an important role in pathways based on their positions in these pathways (Figure 2B, Supplementary Table S3).

Phospholipid remodeling in GBM. In the present study, phospholipid remodeling was demonstrated in GBM (Figure 3A). The phospholipids in GBM were significantly different from those in LGG ($p<0.05$, Figures 3B–3D). Notably, phospholipids species levels which consist of monounsaturated and polyunsaturated fatty acids such as PC (18:0/18:1) and PE (18:2/18:3) were significantly decreased in GBM compared to LGG (Figure 3C). The majority of intermediaries in phospholipid remodeling were shown to be significantly different between LGG and GBM ($p<0.05$, Figure 3D). LPC, lysophosphatidylethanolamine (LPE), and lysophosphatidic acid (LPA) levels were decreased in GBM compared with LGG (Figure 3D).

The expression of key enzymes for phospholipid remodeling was significantly different between GBM and LGG, as indicated by RNA sequencing. The expression of the gene encoding LPCAT1, which selectively incorporates saturated fatty acids into PCs/PEs, was upregulated in GBM compared to LGG (Figure 3B). The expression of the gene encoding LPCAT4 (also called MBOAT2), which selectively incorporates unsaturated fatty acids into PCs/PEs, was downregulated in GBM compared to LGG (Figure 3B). In addition, the expression of enzymes encoding phospholipid biosynthesis GPAT2 and CEPT was upregulated in GBM compared with LGG ($p<0.05$, Figure 3B).

Cellular FA pool in phospholipid metabolism in GBMs. FAs are primary substrates for phospholipid metabolism. *De novo* FA synthesis was increased in GBM to form a cellular pool of saturated and monounsaturated FAs (sFAs and MUFAs, respectively). FAs are *de novo* synthesized from cytoplasmic acetyl-CoA (Figure 4A). In this study, the expression levels of ACLY, IDH1, and ACSS3, which are involved in acetyl-CoA generation from citrate, glutamine, or acetate, were upregulated in GBM compared to those in LGG, as indicated by RNA sequencing (Figure 4C). Acetyl-CoA is then catalyzed to form malonyl-CoA and saturated FA palmitate. Palmitate is then elongated by fatty acid elongases (ELOVL) to form a cellular pool of FAs. Our results also showed that the gene expression of ELOVL2 was upregulated in GBM compared to LGG (Figure 4C).

In addition to *de novo* synthesis, polyunsaturated fatty acids (PUFAs) are essential and must be taken up through multiple routes, including fatty acid-binding proteins

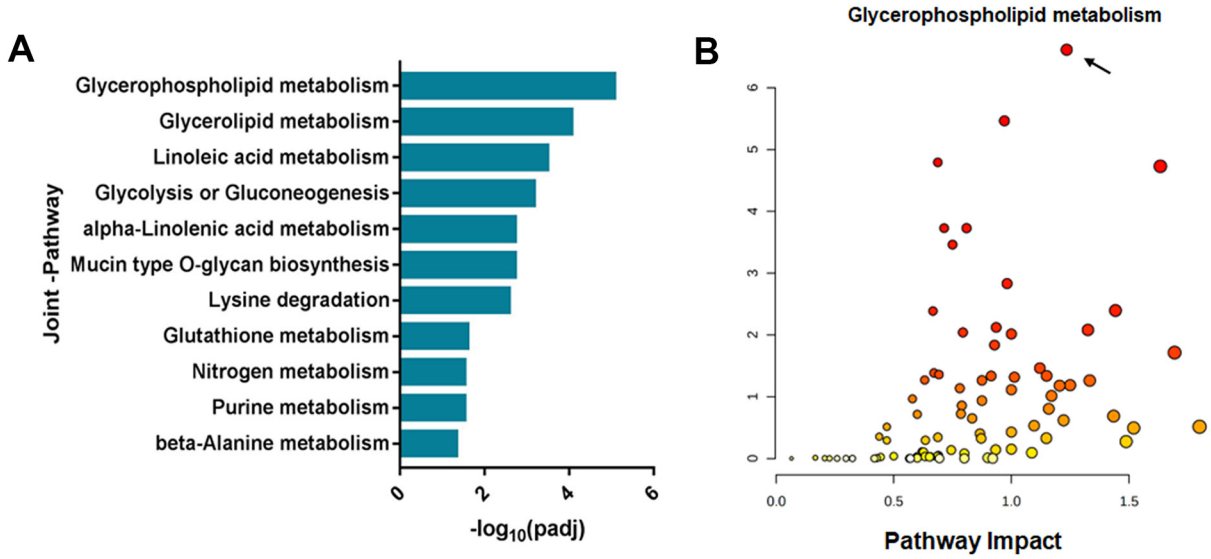

Figure 2. Joint pathway analysis of metabolite-gene correlations between LGGs and GBMs. A) displays the joint pathways that were significantly enriched from the differentially expressed genes and metabolites using the enrichment analysis. B) shows the differentially expressed genes or metabolites that play an important role in joint pathways based on their positions within the pathways.

(FABPs). In this study, the expression levels of FABP5 and FABP7 were significantly increased in GBM compared to those in LGG (Figure 4C). Essential FAs, including alpha-linolenic acid and eicosapentaenoic acid, were found to be significantly increased in GBM compared to LGG (Figure 4B). In addition, the monounsaturated fatty acid such as palmitoleic acid was demonstrated to be significantly increased in GBM compared to LGG (Figure 4B).

The effect of AURKA on phospholipid remodeling in GBM. Patients with GBM were divided into two groups (AURKA_high and AURKA_low) according to the expression level of AURKA. Twenty-six metabolites were significantly different between the AURKA_high and the AURKA_low groups ($p<0.05$). The levels of phospholipids including polyunsaturated fatty acids such as PE (18:0/22:6) were significantly increased in the AURKA_high groups compared

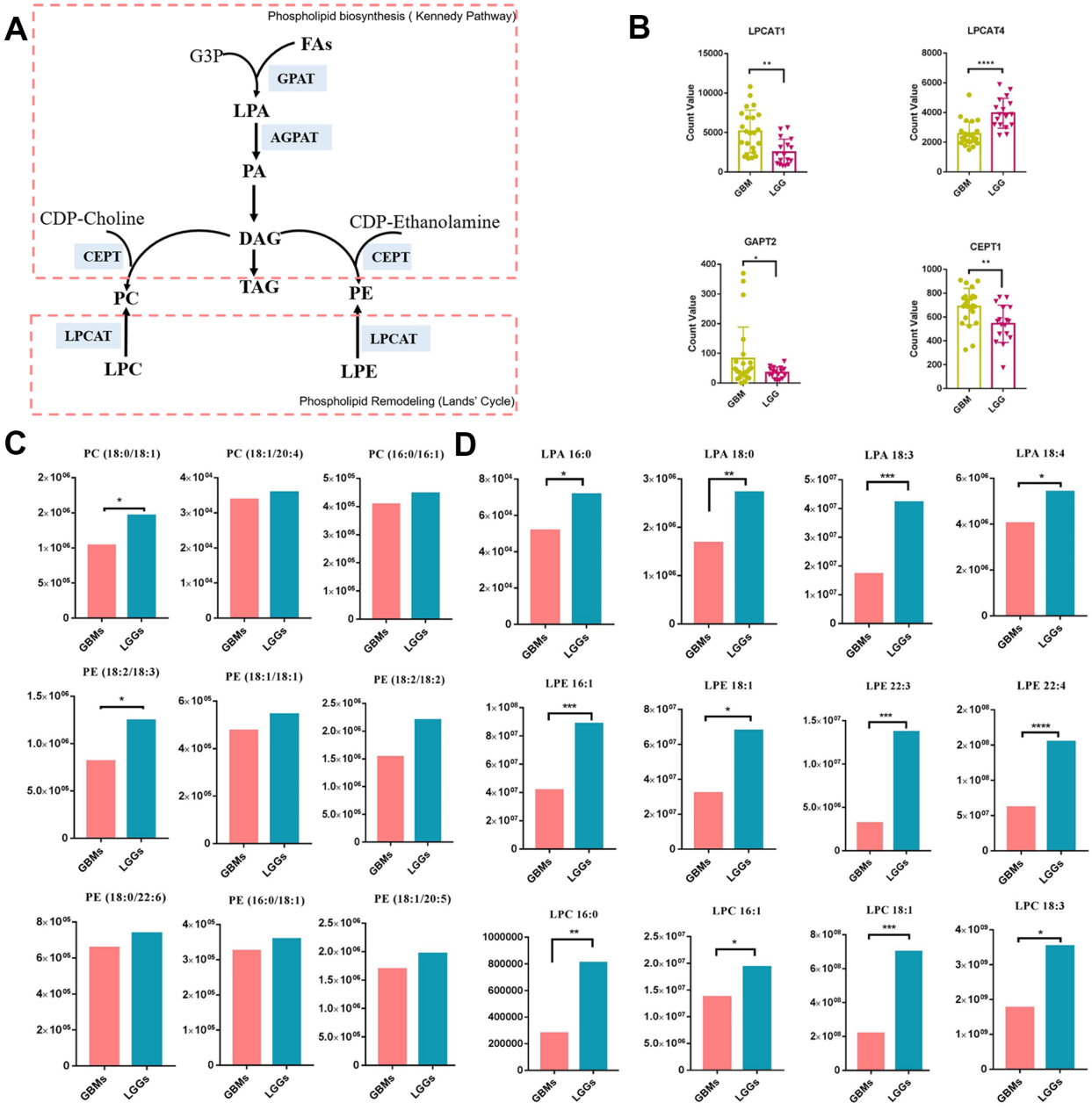

Figure 3. Phospholipid metabolism in GBMs. A) The pathway of phospholipid metabolism. B) Genes that regulate phospholipid metabolism are displayed as significantly different between GBM and LGG groups (mean ± SD, *p<0.05, **p<0.01 and ****p<0.0001). C) Unsaturated PC (18:0/18:1) and PE (18:2/18:3) were significantly decreased in GBM compared to LGG (median, *p<0.05). D) The majority of intermediaries in phospholipid remodeling were shown to be significantly different between LGG and GBM (median, *p<0.05, **p<0.01, ***p<0.001, and ****p<0.0001).

to the AURKA_low groups. The majority of phospholipids which consist of monounsaturated and polyunsaturated fatty acids such as PC (16:0/18:1), PC (16:0/16:1), PC (18:1/20:4), PC (20:4/22:6), PE (18:0/20:4), PE (18:1/20:5), PE (16:0/18:1), and PE (18:2/18:3) were shown to be slightly increased in the AURKA_high groups compared to the AURKA_low groups although there was no significant difference in the levels of these phospholipids between the two groups (Figure 5B). The levels of phospholipids including saturated fatty acids such as PC (18:0/18:0) were moderately declined in the AURKA_high groups compared to the AURKA_low groups although there was no significant difference in the levels of these phospholipids between the two groups (Figure 5B).

The inhibition of Aurora A kinase upregulates the expression of LPCAT1 *in vitro*. In this study, RT-qPCR and western blot assays were performed to evaluate the expression level of AURKA in various glioma cell lines, namely, the LN229, U87, U373, TJ905, M059K, and LN18 cell lines. According to the results of the RT-qPCR and western blot assays, the expression of AURKA was the highest in LN18 cells (Figure 6A). Therefore, LN18 cells were selected and stably transfected cells to knock down AURKA gene expression. According to the results of the transfection efficiency assay, AURKA-sh3 had a satisfactory silencing effect on AURKA expression (Figure 6B). When AURKA expression was knocked down in LN18 cells, the expression of LPCAT1 was significantly elevated (Figure 6D).

To determine the effect of the inhibition of Aurora A kinase on LPCAT1 expression and tumor proliferation, LN18 human GBM cells were after treatment with Aurora A kinase inhibitor-Alisertib, AT9283, and AMG900 for 72 h. The results showed the Aurora kinase A inhibitors exhibited promising anti-proliferative effects on LN18 cells (Figure 6E). Furthermore, LPCAT1 expression was also significantly increased with Aurora kinase A inhibitor-Alisertib, AT9283, and AMG900 treatment for 72 h according to western blot assays and qPCR (Figure 6C).

Aurora A kinase inhibitor upregulates the expression of LPCAT1 *in vivo*. In this study, Alisertib, an inhibitor of Aurora A kinase was used to test the expression of LPCAT1 *in vivo*. C57BL/6 intracranial allograft models were established by intracranial injection of GL261-luc cells in this study. After the tumor formed, the tumor-bearing mice in the control group did not receive any treatment, and the tumor-bearing mice in the Alisertib treatment group received Alisertib every day. After three weeks, the mice treated with Alisertib exhibited smaller tumor sizes compared to those in the control group, there was statistical significance (p=0.0281, Figure 7A). Furthermore, we performed LPCAT1 staining of GL261 tumor sections after Alisertib administration. LPCAT1 staining scores were significantly increased in Alisertib-treated groups compared with untreated groups (Figures 7B, 7C). Together, these animal studies demonstrate that Alisertib suppresses tumor growth and upregulates the expression of LPCAT1 *in vivo*.

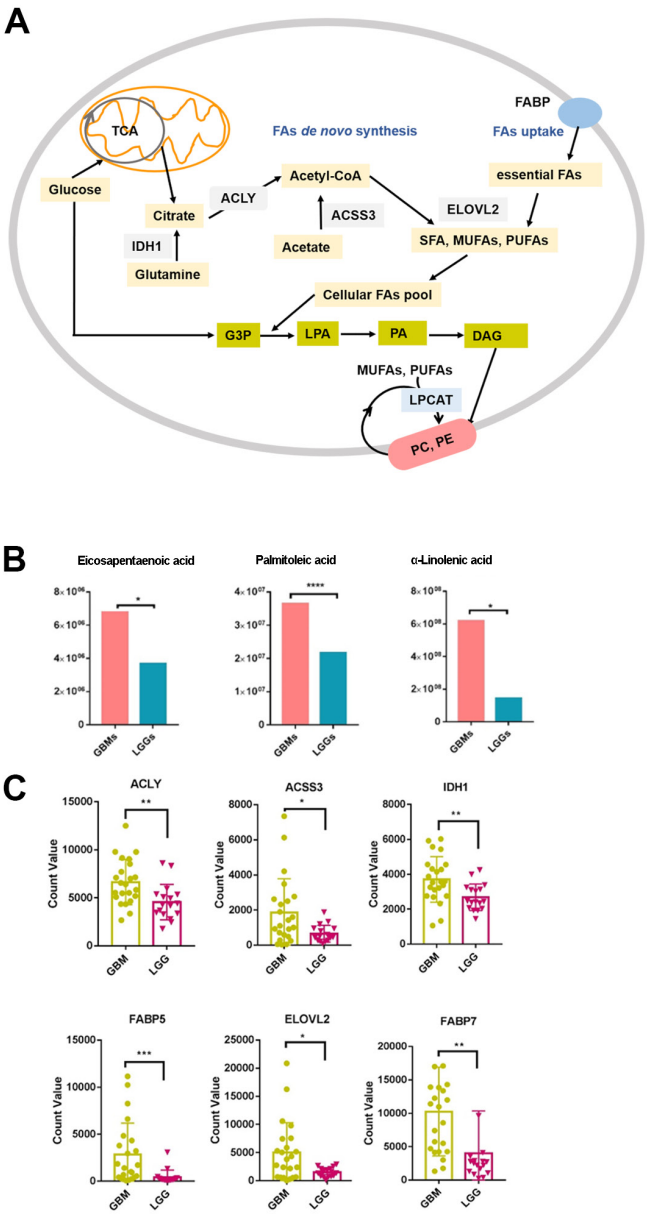

Figure 4. Fatty acid (FA) synthesis changes in GBMs. A) The summary of saturated, monounsaturated FAs, and polyunsaturated FAs metabolic pathways and phospholipid metabolism. B, C) displayed significantly different metabolites and genes expression between GBMs and LGGs (median and mean±SD, *p<0.05, **p<0.01, ***p<0.001, and ****p<0.0001).

Discussion

Lipid metabolism, especially phospholipid metabolism, is significantly altered in various types of cancers, including GBM. However, the roles and mechanisms of phospholipid remodeling in GBM are poorly understood. An integrative analysis coupling global metabolomic with RNA sequencing data was performed to both define and provide molecular context for phospholipid reprogramming in GBM. We identi-

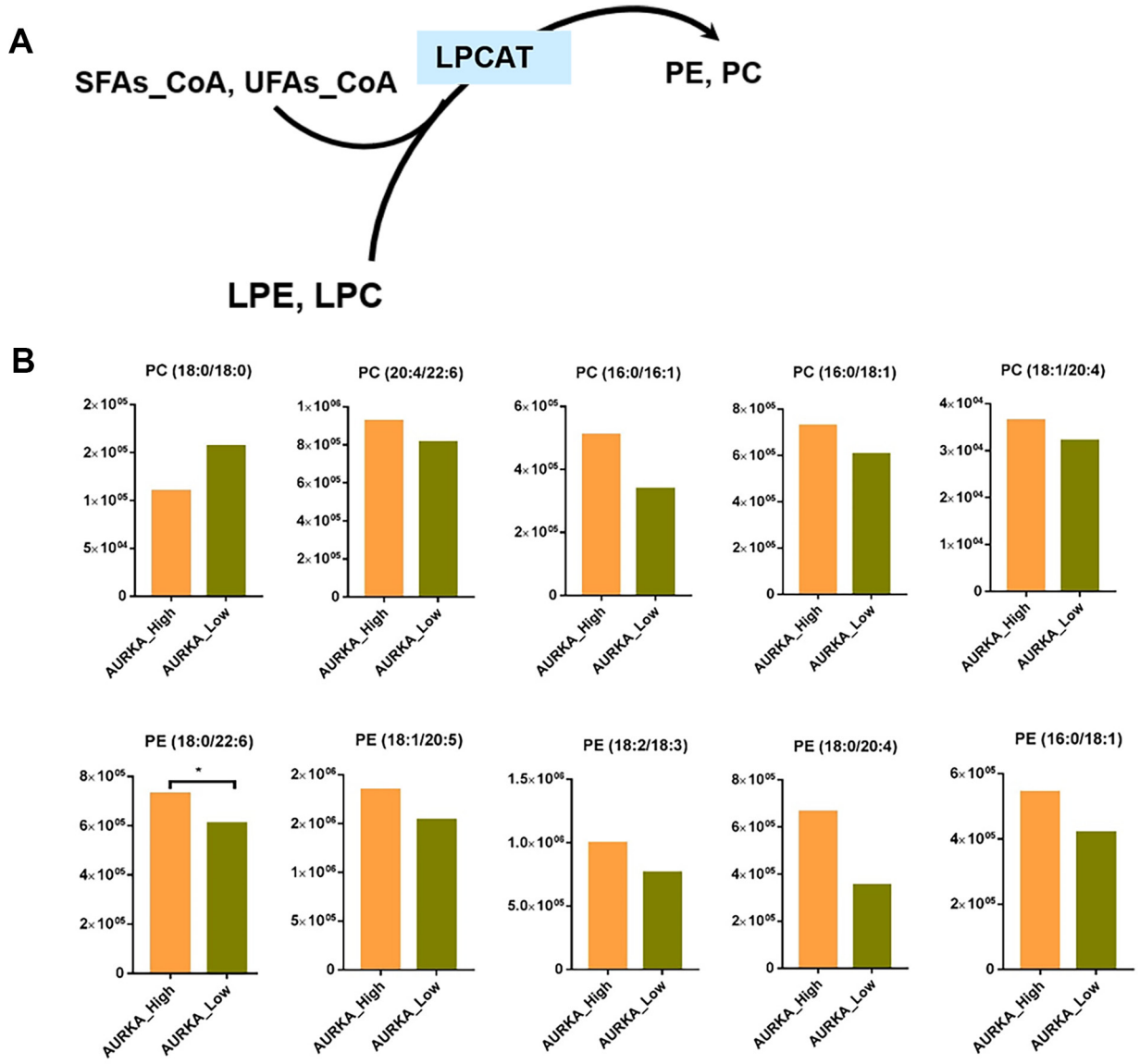

Figure 5. Phospholipid remodeling in GBMs with AURKA high expression. A) The summary of phospholipid (PC and PE) remodeling. B) displayed the different metabolites between GBMs with high AURKA expression and those with low AURKA expression (median, *p<0.05).

fied distinct metabolic signatures when comparing GBM with LGG and discovered a transcriptional program that supported the observed metabolic phenotype. Aberrant phospholipid metabolism was found to be a dominant abnormal metabolic phenotype in GBM, and GBM tumors appeared to co-opt a variety of mechanisms to support its metabolic state, contributing to GBM survival and malignancy.

In cancer cells, the membrane lipid composition often dramatically differs from that of normal cells, and this difference is driven by the dysregulation of enzymes involved in lipid metabolism. One important role of membrane lipid saturation and the relative depletion of polyunsaturated lipid species is the protection of cancer cells from oxidative stress-induced cell death [10, 13, 14]. Studies with several cancer cells have shown that glycerophospholipids containing unsaturated fatty acyl chains appear to be reduced to a certain degree [12, 15]. In this study, we did not find a difference in the membrane lipid composition between GBM and normal brain tissue cells because it was difficult to obtain normal brain tissues. However, our results indicated that the unsaturated lipid composition was significantly decreased in GBM cell membranes compared with LGG cell membranes; these lipids included PC (18:0/18:1) and PE (18:2/18:3) species. Membrane phospholipid composition is important in determining the signaling properties of the plasma membrane of cancer cells by regulating interactions between signaling

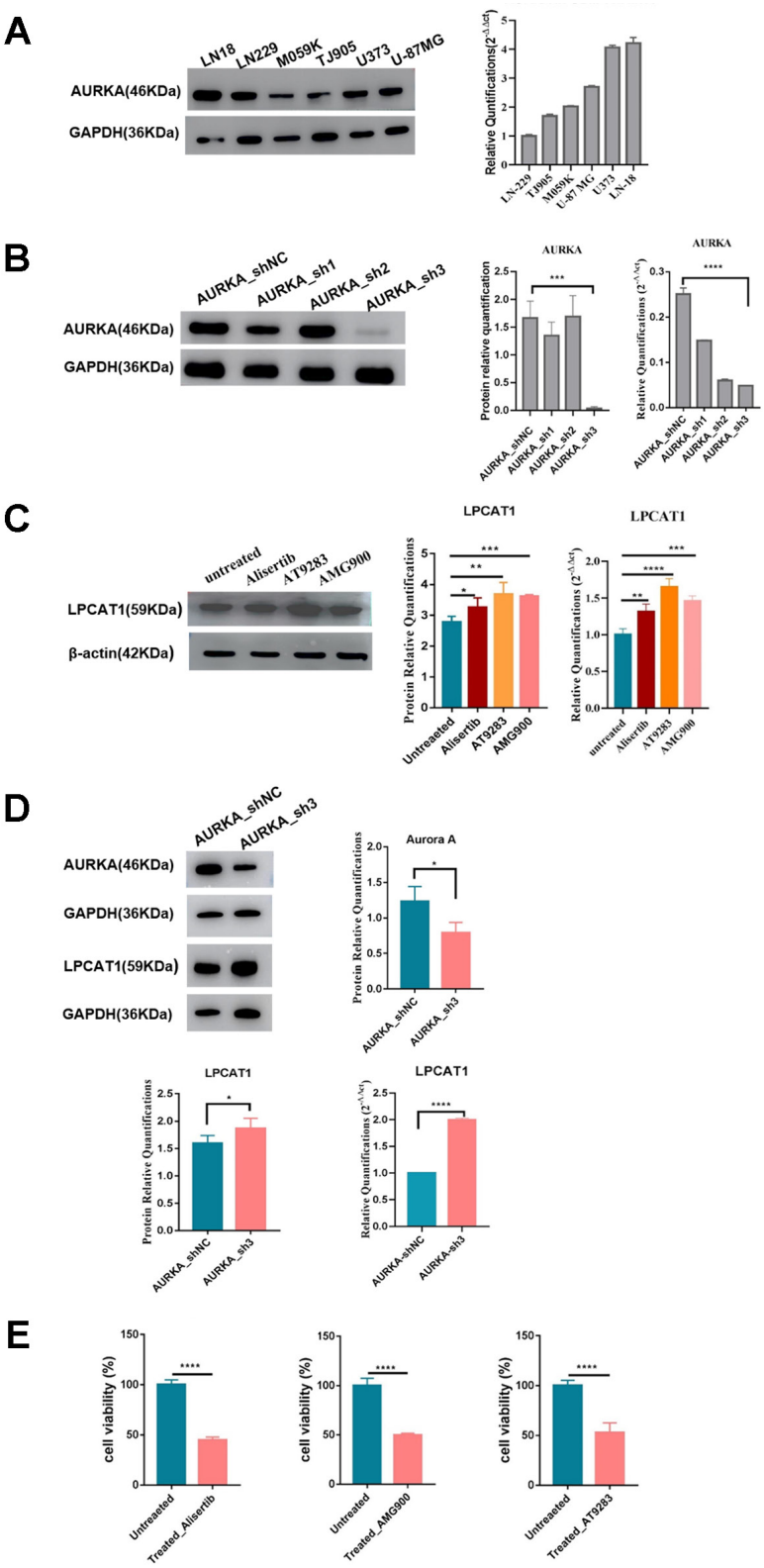

Figure 6. The inhibition of Aurora A kinase upregulates the expression of LPCAT1 in GBM cell lines. A) The mRNA and protein expression level of AURKA in different glioma cell lines. B) The mRNA and protein expression level of AURKA after shRNA_AURKA silencing. C) The LPCAT1 mRNA and protein expression after Alisertib, AT9283, and AMG900 for 72 h. D) The LPCAT1 mRNA and protein expression after AURKA was knocked down. E. The proliferation of LN18 human GBM cells after the Aurora kinase A inhibitors (mean ± SD, *p<0.05, **p<0.01, ***p<0.001, and ****p<0.0001).

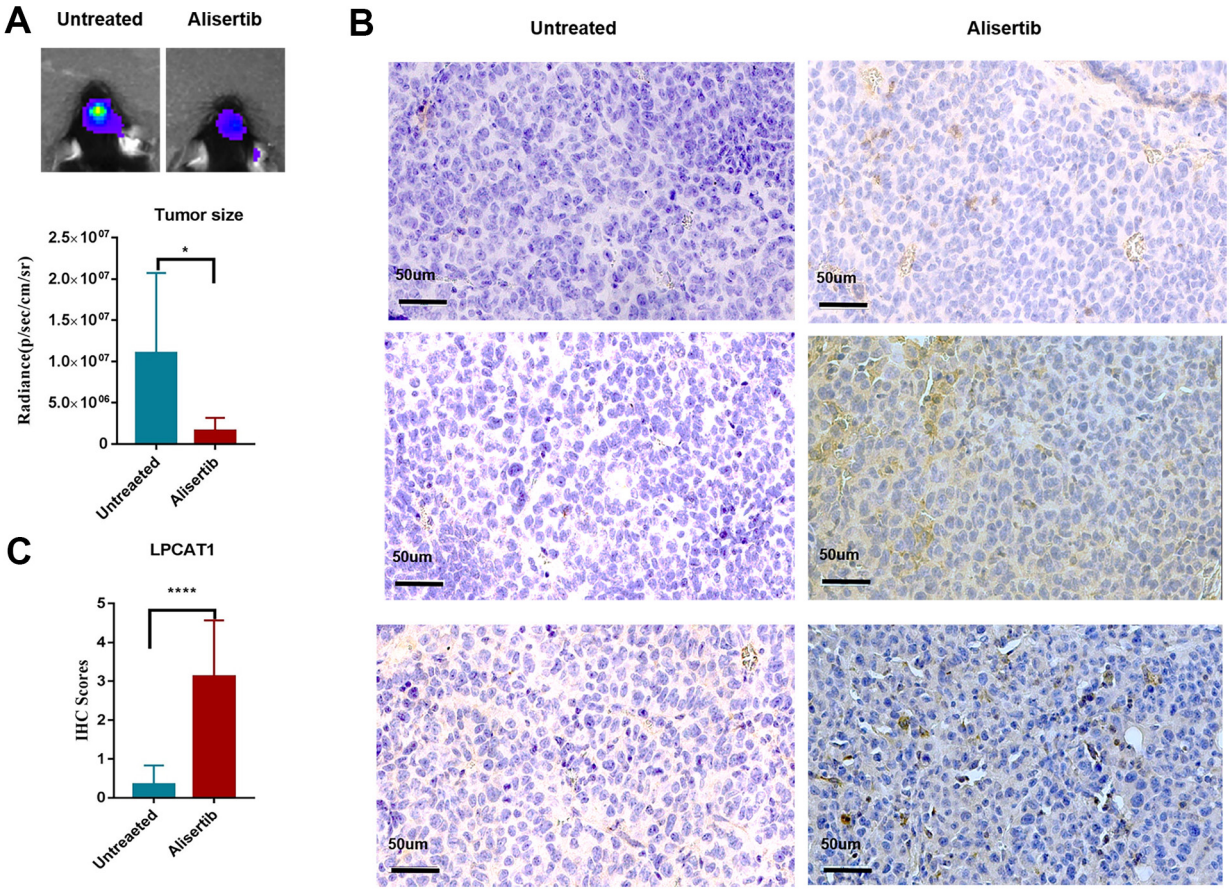

Figure 7. Alisertib upregulates the expression of LPCAT1 in the mouse intracranial model. A) The IVIS system showed tumor size for the untreated and Alisertib-treated groups. B) IHC indicated the LPCAT1 expression for the untreated and Alisertib-treated groups. C) The quantification of LPCAT1 expression between the untreated and Alisertib-treated groups (mean ± SD, ****p<0.0001).

proteins [16, 17]. Saturated phospholipids are critical for permitting proliferative signaling and tumor growth [12]. LPCATs, which catalyze the conversion of 1-acyl-sn-glycerol-3-phosphocholine to 1,2-diacyl-sn-glycerol-3-phosphocholine by incorporating an acyl moiety at the sn-2 position of the glycerol backbone, are specific for regulating membrane phospholipid composition. In the present study, the expression of LPCATs was demonstrated to be significantly different between GBM and LGG. The expression of the LPCAT1 gene, which prefers saturated fatty acyl-CoAs as acyl donors [18], was increased in GBM compared to LGG. Additionally, LPCAT4, which prefers polyunsaturated fatty acyl-CoAs as substrates [19], was decreased in GBM compared to LGG. These results were consistent with those of previous studies demonstrating that LPCAT1 is required for generating these saturated PCs in cancer [12]. Additionally, the integrative analysis from our metabolomic and RNA sequencing data indicated that fatty acid synthesis and uptake were upregulated in GBM compared to LGG, providing acyl groups that contributed to the diverse membrane lipid composition and supported tumorigenesis. In summary, our data indicated that phospholipid metabolism is reprogrammed and the membrane lipid composition differs in GBMs. Furthermore, the abundance of monosaturated and polyunsaturated lipids was decreased in GBM, and thus, the abundance of saturated lipids was increased in GBM. These results are consistent with those of previous studies, suggesting the complex interplay of different LPCATs in determining the aggressive behavior of cancer cells, which is mediated by the regulation of PC saturation to control membrane structure and signaling activity [14, 20, 21].

AURKA is generally recognized as an oncogene due to its upregulation in a variety of tumor tissues, including GBM [22, 23]. Aurora kinases have attracted attention owing to their broad functions in the cell cycle, DNA damage response, and apoptosis, as well as their upregulated expression in various types of cancer and the inverse correlation between Aurora kinase expression and patient prognosis. Aurora A kinase inhibitors have been demonstrated to suppress the proliferation of multiple types of

cancers in preclinical and clinical studies [24-27]. We initially sought to identify kinase inhibitors that could affect lipid-modifying enzymes, therefore contributing to plasma membrane remodeling and influencing the interaction of signaling proteins in GBM. Our metabolic profiling data showed that the abundance of unsaturated PCs and PEs was increased in GBM with high AURKA expression compared with GBM with low AURKA expression, and the abundance of saturated PCs and PEs was decreased in GBM with high AURKA expression compared with GBM with low AURKA expression; however, the sample size was too small. Intriguingly, our experimental results for GBM cell lines first showed that Aurora A kinase siRNA and inhibitors–Alisertib, AMG900, and AT9238 induced an increase in LPCAT1 mRNA and protein expression *in vitro* and *in vivo*, at least potentially influencing membrane lipid remodeling and signaling pathways in GBM. Previous studies indicated LPCAT1 regulated saturated membrane phospholipid composition and tumorigenesis [12, 14, 20, 21]. LPCAT1 was shown as a critical node integrating EGFR signaling with lipid remodeling to alter the physical properties of the plasma membrane and create a protumor cellular state [12]. However, the mechanism of AURKA regulating LPCAT1 expression was still unknown. Studies demonstrated that AURKA siRNA or pharmacological inhibition decreased GSK-3β protein and its phosphorylation level [23, 28]. Moreover, GSK-3β could phosphorylate LPCAT1 and subsequently signal its polyubiquitination and proteolysis [29]. Silencing of the GSK-3β gene reduced LPCAT1 degradation and increased the LPCAT1 protein level [29]. In a word, we considered the reasons for Aurora-A inhibition-induced LPCAT1 expression level are still complex; therefore, the exact mechanism needs to be further explored.

In addition, we found AURKA inhibition not only suppressed GBM cell proliferation but also increased LPCAT1 expression. However, LPCAT1 was found to promote cancer cell survival and progression in various types of cancer [4, 30]. Thus, we hypothesized that the inhibition of AURKA on GBM proliferation is independent of LPCAT1 function, which is more conducive to improving the therapeutic efficacy of AURKA inhibition combined with LPCAT1 inhibitor in the treatment of GBM. To our knowledge, low molecular weight LPCAT1 inhibitors are not commercially available to be used in this study. The combination therapeutic effect of AURKA inhibition with LPCAT1 inhibitor should be carried out in future studies.

In summary, our results showed that phospholipid remodeling caused a reduction in the polyunsaturated membrane lipid composition in GBM. Aurora A kinase inhibition increased LPCAT1 expression and suppressed GBM cell proliferation. The AURKA inhibitors-Alisertib, AMG900, and AT9283 not only exerted antitumor effects but also induced LPCAT1 expression. In the future, Aurora kinase inhibition combined with LPCAT1 inhibition may be used to exert promising synergistic effects on GBM.

Supplementary information is available in the online version of the paper.

Acknowledgments: Shuyu Hao is supported by the National Natural Science Foundation of China (81872052). Nan Ji is supported by the National Natural Science Foundation of China (81930048) and the Capital Health Research and Development of Special (2022-2-2047). Jie Feng is supported by the National Natural Science Foundation of China (81702455).

References

[1] HUANG T, CHENG SY. Targeting phospholipid metabolism for glioblastoma therapy. Neuro Oncol 2021; 23: 343–344. https://doi.org/10.1093/neuonc/noaa309

[2] VAN MEER G, VOELKER DR, FEIGENSON GW. Membrane lipids: where they are and how they behave. Nat Rev Mol Cell Biol 2008; 9: 112–124. https://doi.org/10.1038/nrm2330

[3] WYMANN MP, SCHNEITER R. Lipid signalling in disease. Nat Rev Mol Cell Biol 2008; 9: 162–176. https://doi.org/10.1038/nrm2335

[4] WANG B, TONTONOZ P. Phospholipid Remodeling in Physiology and Disease. Annual review of physiology 2019; 81: 165–188. https://doi.org/10.1146/annurev-physiol-020518-114444

[5] SPECTOR AA, YOREK MA. Membrane lipid composition and cellular function. J Lipid Res 1985; 26: 1015–1035.

[6] LANDS WE. Metabolism of glycerolipides; a comparison of lecithin and triglyceride synthesis. J Biol Chem 1958; 231: 883–888.

[7] MERKL I, LANDS WE. Metabolism of glycerolipids. IV. Synthesis of phosphatidylethanolamine. J Biol Chem 1963; 238: 905–906.

[8] SNAEBJORNSSON MT, JANAKI-RAMAN S, SCHULZE A. Greasing the Wheels of the Cancer Machine: The Role of Lipid Metabolism in Cancer. Cell Metab 2020; 31: 62–76. https://doi.org/10.1016/j.cmet.2019.11.010

[9] MACDONALD JI, SPRECHER H. Phospholipid fatty acid remodeling in mammalian cells. Biochim Biophys Acta 1991; 1084: 105–121. https://doi.org/10.1016/0005-2760(91)90209-z

[10] RYSMAN E, BRUSSELMANS K, SCHEYS K, TIMMERMANS L, DERUA R, et al. De novo lipogenesis protects cancer cells from free radicals and chemotherapeutics by promoting membrane lipid saturation. Cancer Res 2010; 70: 8117–8126. https://doi.org/10.1158/0008-5472.CAN-09-3871

[11] AKAGI S, KONO N, ARIYAMA H, SHINDOU H, SHIMIZU T et al. Lysophosphatidylcholine acyltransferase 1 protects against cytotoxicity induced by polyunsaturated fatty acids. FASEB J 2016; 30: 2027–2039. https://doi.org/10.1096/fj.201500149

[12] BI J, ICHU TA, ZANCA C, YANG H, ZHANG W et al. Oncogene Amplification in Growth Factor Signaling Pathways Renders Cancers Dependent on Membrane Lipid Remodeling. Cell Metab 2019; 30: 525–538 e528. https://doi.org/10.1016/j.cmet.2019.06.014

[13] SWINNEN JV, DEHAIRS J, TALEBI A. Membrane Lipid Remodeling Takes Center Stage in Growth Factor Receptor-Driven Cancer Development. Cell metabolism 2019; 30: 407–408. https://doi.org/10.1016/j.cmet.2019.08.016

[14] PINOT M, VANNI S, PAGNOTTA S, LACAS-GERVAIS S, PAYET LA et al. Lipid cell biology. Polyunsaturated phospholipids facilitate membrane deformation and fission by endocytic proteins. Science 2014; 345: 693–697. https://doi.org/10.1126/science.1255288

[15] HILVO M, DENKERT C, LEHTINEN L, MULLER B, BROCKMOLLER S et al. Novel theranostic opportunities offered by characterization of altered membrane lipid metabolism in breast cancer progression. Cancer Res 2011; 71: 3236–3245. https://doi.org/10.1158/0008-5472.CAN-10-3894

[16] ARKHIPOV A, SHAN Y, DAS R, ENDRES NF, EASTWOOD MP et al. Architecture and membrane interactions of the EGF receptor. Cell 2013; 152: 557–569. https://doi.org/10.1016/j.cell.2012.12.030

[17] ZHOU Y, PRAKASH P, LIANG H, CHO KJ, GORFE AA et al. Lipid-Sorting Specificity Encoded in K-Ras Membrane Anchor Regulates Signal Output. Cell 2017; 168: 239–251 e216. https://doi.org/10.1016/j.cell.2016.11.059

[18] NAKANISHI H, SHINDOU H, HISHIKAWA D, HARAYAMA T, OGASAWARA R et al. Cloning and characterization of mouse lung-type acyl-CoA:lysophosphatidylcholine acyltransferase 1 (LPCAT1). Expression in alveolar type II cells and possible involvement in surfactant production. J Biol Chem 2006; 281: 20140–20147. https://doi.org/10.1074/jbc.M600225200

[19] HISHIKAWA D, SHINDOU H, KOBAYASHI S, NAKANISHI H, TAGUCHI R et al. Discovery of a lysophospholipid acyltransferase family essential for membrane asymmetry and diversity. Proc Natl Acad Sci U S A 2008; 105: 2830–2835. https://doi.org/10.1073/pnas.0712245105

[20] HASHIDATE-YOSHIDA T, HARAYAMA T, HISHIKAWA D, MORIMOTO R, HAMANO F et al. Fatty acid remodeling by LPCAT3 enriches arachidonate in phospholipid membranes and regulates triglyceride transport. Elife 2015; 4: e06328. https://doi.org/10.7554/eLife.06328

[21] WANG B, RONG X, PALLADINO END, WANG J, FOGELMAN AM et al. Phospholipid Remodeling and Cholesterol Availability Regulate Intestinal Stemness and Tumorigenesis. Cell Stem Cell 2018; 22: 206–220 e204. https://doi.org/10.1016/j.stem.2017.12.017

[22] WILLEMS E, LOMBARD A, DEDOBBELEER M, GOFFART N, ROGISTER B. The Unexpected Roles of Aurora A Kinase in Gliobastoma Recurrences. Target Oncol 2017; 12: 11–18. https://doi.org/10.1007/s11523-016-0457-2

[23] NGUYEN TTT, SHANG E, SHU C, KIM S, MELA A et al. Aurora kinase A inhibition reverses the Warburg effect and elicits unique metabolic vulnerabilities in glioblastoma. Nat Commun 2021; 12: 5203. https://doi.org/10.1038/s41467-021-25501-x

[24] YAN M, WANG C, HE B, YANG M, TONG M et al. Aurora-A Kinase: A Potent Oncogene and Target for Cancer Therapy. Med Res Rev 2016; 36: 1036–1079. https://doi.org/10.1002/med.21399

[25] TANG A, GAO K, CHU L, ZHANG R, YANG J et al. Aurora kinases: novel therapy targets in cancers. Oncotarget 2017; 8: 23937–23954. https://doi.org/10.18632/oncotarget.14893

[26] VAN BROCKLYN JR, WOJTON J, MEISEN WH, KELLOUGH DA, ECSEDY JA et al. Aurora-A inhibition offers a novel therapy effective against intracranial glioblastoma. Cancer Res 2014; 74: 5364–5370. https://doi.org/10.1158/0008-5472.Can-14-0386

[27] KUROKAWA C, GEEKIYANAGE H, ALLEN C, IANKOV I, SCHROEDER M et al. Alisertib demonstrates significant antitumor activity in bevacizumab resistant, patient derived orthotopic models of glioblastoma. J Neurooncol 2017; 131: 41–48. https://doi.org/10.1007/s11060-016-2285-8

[28] DAR AA, BELKHIRI A, EL-RIFAI W. The aurora kinase A regulates GSK-3beta in gastric cancer cells. Oncogene 2009; 28: 866–875. https://doi.org/10.1038/onc.2008.434

[29] ZOU C, BUTLER PL, COON TA, SMITH RM, HAMMEN G et al. LPS impairs phospholipid synthesis by triggering beta-transducin repeat-containing protein (beta-TrCP)-mediated polyubiquitination and degradation of the surfactant enzyme acyl-CoA:lysophosphatidylcholine acyltransferase I (LPCAT1). J Biol Chem 2011; 286: 2719–2727. https://doi.org/10.1074/jbc.M110.192377

[30] TAO M, LUO J, GU T, YU X, SONG Z et al. LPCAT1 reprogramming cholesterol metabolism promotes the progression of esophageal squamous cell carcinoma. Cell Death Dis 2021; 12: 845. https://doi:10.1038/s41419-021-04132-6

https://doi.org/10.4149/neo_2023_221126N1140

The inhibition of Aurora A kinase regulates phospholipid remodeling by upregulating LPCAT1 in glioblastoma

Ya-Zhou MIAO[1,2,3,#], Jing WANG[1,#], Shu-Yu HAO[1,2], Yu-Xuan DENG[2], Zhe ZHANG[2], Ze-Ping JIN[2], Da-Yuan LIU[2,4], Shao-Dong ZHANG[1], Hong WAN[1], Nan JI[2,5,6,*], Jie FENG[1,*]

Supplementary Information

Supplementary Table S1. Sequences of the primers used for RT-qPCR.

Gene	Forward primer (5'–3')	Reverse primer (5'–3')
LPCAT1	CGCCTCACTCGTCCTACTTC	TTCCCCAGATCGGGATGTCTC
AURKA	GAGGTCCAAAACGTGTTCTCG	ACAGGATGAGGTACACTGGTTG
GAPDH	CTGCTGATGCCCCCATGTTC	ACCTTGGCCAGGGGTGCTAA

Supplementary Table S2. The enrichment analysis of the identified genes and metabolites in GBM.

	Total	Expected	Hits	Raw p	Holm adjust	FDR	Impact
Glycerophospholipid metabolism	86	21.535	44	1.02E-07	8.55E-06	8.55E-06	1.2353
Glycerolipid metabolism	35	8.7643	22	2.09E-06	0.00017	8.76E-05	0.97059
Linoleic acid metabolism	17	4.257	13	1.17E-05	0.00096	0.00033	0.6875
Glycolysis or Gluconeogenesis	61	15.275	30	3.26E-05	0.00264	0.00068	1.5333
alpha-Linolenic acid metabolism	22	5.509	14	0.00014	0.0109	0.00191	0.71429
Mucin type O-glycan biosynthesis	22	5.509	14	0.00014	0.0109	0.00191	0.80952
Lysine degradation	49	12.27	24	0.00022	0.01719	0.00265	0.75
Glutathione metabolism	56	14.023	24	0.00241	0.18554	0.0253	0.90909
Nitrogen metabolism	10	2.5041	7	0.00347	0.26407	0.02939	0.66667
Purine metabolism	166	41.568	57	0.0035	0.26407	0.02939	1.3636
beta-Alanine metabolism	44	11.018	19	0.00607	0.44922	0.04636	1.3256
Arginine biosynthesis	27	6.7611	13	0.00758	0.55311	0.05304	1
Starch and sucrose metabolism	43	10.768	18	0.01094	0.78758	0.07068	0.92857
Inositol phosphate metabolism	69	17.278	26	0.01249	0.88649	0.07491	0.77941
Histidine metabolism	32	8.0131	14	0.01549	1	0.08677	0.90323
Pantothenate and CoA biosynthesis	34	8.5139	14	0.02759	1	0.14482	1.1212
N-Glycan biosynthesis	77	19.282	27	0.02984	1	0.14743	0.67105
Cysteine and methionine metabolism	71	17.779	25	0.03405	1	0.15322	0.91429
Alanine, aspartate and glutamate metabolism	61	15.275	22	0.03466	1	0.15322	1.15
Thiamine metabolism	14	3.5057	7	0.03815	1	0.16023	0.69231
Ether lipid metabolism	39	9.766	15	0.04314	1	0.17254	0.63158
Neomycin, kanamycin and gentamicin biosynthesis	4	1.0016	3	0.05087	1	0.19422	1.3333
Phosphatidylinositol signaling system	74	18.53	25	0.05506	1	0.19982	0.78082
Pyrimidine metabolism	99	24.791	32	0.05872	1	0.19982	1.4592
Arginine and proline metabolism	78	19.532	26	0.05947	1	0.19982	0.97403
Glycosaminoglycan biosynthesis - heparan sulfate / heparin	7	1.7529	4	0.07065	1	0.22826	1
Nicotinate and nicotinamide metabolism	42	10.517	15	0.07968	1	0.24789	1.1707
Drug metabolism - other enzymes	70	17.529	23	0.08462	1	0.25387	0.57971
Arachidonic acid metabolism	81	20.283	26	0.08911	1	0.2581	0.875
Fructose and mannose metabolism	40	10.016	14	0.10252	1	0.28705	1.0769
Sphingolipid metabolism	58	14.524	19	0.11307	1	0.30639	0.78947
Phenylalanine metabolism	21	5.2586	8	0.12991	1	0.34102	1.2
Riboflavin metabolism	9	2.2537	4	0.16611	1	0.41086	0.5
Butanoate metabolism	29	7.2619	10	0.1663	1	0.41086	0.78571
Ascorbate and aldarate metabolism	13	3.2553	5	0.20655	1	0.49573	0.83333

Supplementary Table S2. ***Continued . . .***

	Total	Expected	Hits	Raw p	Holm adjust	FDR	Impact
Pyruvate metabolism	45	11.268	14	0.21591	1	0.50379	1.0909
Synthesis and degradation of ketone bodies	10	2.5041	4	0.22472	1	0.51018	1.2222
Pentose and glucuronate interconversions	32	8.0131	10	0.26402	1	0.56171	1.0968
Pentose phosphate pathway	47	11.769	14	0.27235	1	0.56171	1.2174
Terpenoid backbone biosynthesis	36	9.0148	11	0.27559	1	0.56171	0.54286
Galactose metabolism	51	12.771	15	0.28025	1	0.56171	1.52
Glycosaminoglycan biosynthesis - chondroitin sulfate / dermatan sulfate	18	4.5074	6	0.28343	1	0.56171	0.47059
Phenylalanine, tyrosine and tryptophan biosynthesis	11	2.7545	4	0.28754	1	0.56171	1.8
Valine, leucine and isoleucine biosynthesis	12	3.0049	4	0.35233	1	0.67264	1
Taurine and hypotaurine metabolism	16	4.0066	5	0.37111	1	0.69274	0.86667
Aminoacyl-tRNA biosynthesis	74	18.53	20	0.38827	1	0.70902	0.43836
Propanoate metabolism	48	12.02	13	0.42554	1	0.74845	1.1489
Ubiquinone and other terpenoid-quinone biosynthesis	17	4.257	5	0.42769	1	0.74845	0.6875
Porphyrin and chlorophyll metabolism	53	13.272	14	0.4607	1	0.78977	0.63462
Sulfur metabolism	18	4.5074	5	0.48317	1	0.80835	0.47059
Citrate cycle (TCA cycle)	42	10.517	11	0.49078	1	0.80835	1.4878
Amino sugar and nucleotide sugar metabolism	79	19.782	20	0.52147	1	0.84238	0.79487
Retinol metabolism	47	11.769	11	0.65842	1	1	1.087
Glycine, serine and threonine metabolism	68	17.028	16	0.66087	1	1	1
Glycosphingolipid biosynthesis - globo and isoglobo series	31	7.7627	7	0.69156	1	1	0.93333
Glycosaminoglycan degradation	44	11.018	10	0.69551	1	1	0.74419
Valine, leucine and isoleucine degradation	88	22.036	20	0.73353	1	1	0.62069
D-Glutamine and D-glutamate metabolism	10	2.5041	2	0.75747	1	1	0.55556
Tryptophan metabolism	84	21.034	18	0.81657	1	1	0.61446
D-Arginine and D-ornithine metabolism	6	1.5025	1	0.82297	1	1	0.8
Selenocompound metabolism	35	8.7643	6	0.90493	1	1	0.5
Various types of N-glycan biosynthesis	36	9.0148	6	0.91893	1	1	0.68571
Glycosylphosphatidylinositol (GPI)-anchor biosynthesis	31	7.7627	5	0.91934	1	1	0.63333
Glyoxylate and dicarboxylate metabolism	56	14.023	10	0.92539	1	1	0.65455
Glycosphingolipid biosynthesis - ganglio series	47	11.769	8	0.93194	1	1	0.65217
Phosphonate and phosphinate metabolism	10	2.5041	1	0.94434	1	1	0.44444
Caffeine metabolism	19	4.7578	2	0.96971	1	1	0.16667
One carbon pool by folate	31	7.7627	4	0.97036	1	1	0.9
Tyrosine metabolism	88	22.036	15	0.97445	1	1	0.62069
Vitamin B6 metabolism	21	5.2586	2	0.98151	1	1	0.4
Folate biosynthesis	61	15.275	9	0.98327	1	1	0.6
Lipoic acid metabolism	15	3.7561	1	0.98694	1	1	0.42857
Mannose type O-glycan biosynthesis	30	7.5123	3	0.98988	1	1	0.2069
Drug metabolism - cytochrome P450	98	24.54	15	0.99381	1	1	0.2268
Biotin metabolism	21	5.2586	1	0.99772	1	1	0.8
Fatty acid degradation	102	25.542	14	0.99855	1	1	0.92079
Primary bile acid biosynthesis	92	23.038	12	0.99871	1	1	0.41758
Biosynthesis of unsaturated fatty acids	47	11.769	3	0.99984	1	1	0.06522
Steroid biosynthesis	82	20.534	8	0.99989	1	1	0.25926
Metabolism of xenobiotics by cytochrome P450	145	36.309	18	0.99997	1	1	0.69444
Fatty acid biosynthesis	129	32.303	5	1	1	1	0.29688
Fatty acid elongation	75	18.781	3	1	1	1	0.32432
Steroid hormone biosynthesis	199	49.832	15	1	1	1	0.5404
Glycosphingolipid biosynthesis - lacto and neolacto series	121	30.3	11	1	1	1	0.56667

Supplementary Table S3. The topology analysis of the identified genes and metabolites in GBM.

	matched_features
Glycerophospholipid metabolism	cpd:C00350; cpd:C00157; cpd:C00111; cpd:C04230; cpd:C00588; cpd:C01996; cpd:C00346; cpd:C00416; cpd:C00093; hsa:9791; hsa:10162; hsa:79888; hsa:10390; hsa:1103; hsa:100137049; hsa:151056; hsa:283748; hsa:5320; hsa:5321; hsa:5322; hsa:81579; hsa:8398; hsa:8605; hsa:8681; hsa:139189; hsa:9162; hsa:196051; hsa:23175; hsa:64900; hsa:84513; hsa:23646; hsa:129642; hsa:154141; hsa:253558; hsa:56894; hsa:162466; hsa:150763; hsa:57678; hsa:84803; hsa:10434; hsa:11313; hsa:8760; hsa:23659; hsa:64850
Glycerolipid metabolism	cpd:C00416; cpd:C00093; cpd:C00116; cpd:C00111; hsa:196051; hsa:23175; hsa:64900; hsa:84513; hsa:129642; hsa:154141; hsa:253558; hsa:56894; hsa:150763; hsa:57678; hsa:84803; hsa:2710; hsa:2712; hsa:217; hsa:223; hsa:2717; hsa:139189; hsa:9162
Linoleic acid metabolism	cpd:C00157; hsa:1573; hsa:1571; hsa:100137049; hsa:151056; hsa:283748; hsa:5320; hsa:5321; hsa:5322; hsa:81579; hsa:8398; hsa:8605; hsa:8681
Glycolysis or Gluconeogenesis	cpd:C00022; cpd:C00111; hsa:217; hsa:223; hsa:218; hsa:220; hsa:125; hsa:130; hsa:1737; hsa:3939; hsa:3945; hsa:5315; hsa:387712; hsa:2597; hsa:7167; hsa:229; hsa:230; hsa:5211; hsa:5213; hsa:2203; hsa:2821; hsa:55276; hsa:3099; hsa:3101; hsa:130589; hsa:57818; hsa:92579; hsa:5230; hsa:84532; hsa:83440
alpha-Linolenic acid metabolism	cpd:C00157; cpd:C06427; hsa:51; hsa:100137049; hsa:151056; hsa:283748; hsa:5320; hsa:5321; hsa:5322; hsa:81579; hsa:8398; hsa:8605; hsa:8681; hsa:9415
Mucin type O-glycan biosynthesis	hsa:2650; hsa:9334; hsa:55808; hsa:6482; hsa:6483; hsa:11227; hsa:114805; hsa:2589; hsa:2590; hsa:2591; hsa:26290; hsa:79695; hsa:8693; hsa:29071
Lysine degradation	cpd:C00956; cpd:C00408; hsa:8424; hsa:223; hsa:217; hsa:79823; hsa:2145; hsa:2146; hsa:4297; hsa:56950; hsa:64324; hsa:6839; hsa:7468; hsa:80854; hsa:387893; hsa:93166; hsa:79709; hsa:8985; hsa:5351; hsa:5352; hsa:51166; hsa:55526; hsa:2639; hsa:51268
Glutathione metabolism	cpd:C00077; cpd:C00134; cpd:C00315; hsa:290; hsa:51056; hsa:2882; hsa:493869; hsa:51060; hsa:3417; hsa:2936; hsa:2937; hsa:2729; hsa:2730; hsa:26873; hsa:79017; hsa:119391; hsa:2941; hsa:2946; hsa:2947; hsa:373156; hsa:4258; hsa:6611; hsa:6240; hsa:6241
Nitrogen metabolism	hsa:377677; hsa:760; hsa:761; hsa:762; hsa:768; hsa:771; hsa:2746
Purine metabolism	cpd:C04677; cpd:C00008; cpd:C03794; cpd:C00212; cpd:C00559; cpd:C05512; cpd:C00242; cpd:C00499; cpd:C00387; cpd:C00301; cpd:C00366; cpd:C06196; cpd:C04051; hsa:6240; hsa:6241; hsa:5634; hsa:5471; hsa:10606; hsa:50940; hsa:5143; hsa:8622; hsa:108; hsa:111; hsa:112; hsa:114; hsa:84284; hsa:4831; hsa:158067; hsa:203; hsa:204; hsa:205; hsa:22978; hsa:51251; hsa:84618; hsa:132; hsa:4860; hsa:124583; hsa:957; hsa:3614; hsa:8833; hsa:58497; hsa:2984; hsa:3000; hsa:4881; hsa:5145; hsa:5146; hsa:5147; hsa:5148; hsa:5152; hsa:8654; hsa:3704; hsa:5167; hsa:5169; hsa:318; hsa:55276; hsa:2272; hsa:5315
beta-Alanine metabolism	cpd:C00049; cpd:C02642; cpd:C00429; cpd:C01262; cpd:C00106; cpd:C00135; cpd:C00315; hsa:35; hsa:26275; hsa:4329; hsa:18; hsa:57571; hsa:217; hsa:223; hsa:218; hsa:220; hsa:51733; hsa:1806; hsa:51
Arginine biosynthesis	cpd:C00049; cpd:C00077; cpd:C00624; cpd:C00122; hsa:2746; hsa:4843; hsa:4846; hsa:100526760; hsa:162417; hsa:435; hsa:445; hsa:2875; hsa:84706
Starch and sucrose metabolism	cpd:C00092; cpd:C01231; hsa:3099; hsa:3101; hsa:5167; hsa:5169; hsa:283209; hsa:7360; hsa:2997; hsa:55276; hsa:57818; hsa:92579; hsa:2821; hsa:2632; hsa:279; hsa:280; hsa:178; hsa:5836
Inositol phosphate metabolism	cpd:C00092; cpd:C00111; hsa:5305; hsa:8396; hsa:3632; hsa:80271; hsa:3705; hsa:3628; hsa:51477; hsa:3613; hsa:54928; hsa:55586; hsa:55300; hsa:8394; hsa:8897; hsa:9108; hsa:113026; hsa:23236; hsa:51196; hsa:5335; hsa:9651; hsa:5290; hsa:4329; hsa:7167; hsa:5288; hsa:22908
Histidine metabolism	cpd:C00785; cpd:C00135; cpd:C01262; cpd:C00049; hsa:3034; hsa:57571; hsa:3067; hsa:217; hsa:223; hsa:218; hsa:220; hsa:26; hsa:3176; hsa:443
Pantothenate and CoA biosynthesis	cpd:C00864; cpd:C02642; cpd:C00429; cpd:C00183; cpd:C00049; cpd:C00106; hsa:5167; hsa:5169; hsa:80025; hsa:51733; hsa:1806; hsa:8875; hsa:586; hsa:79717
N-Glycan biosynthesis	hsa:8813; hsa:144245; hsa:84920; hsa:79053; hsa:29929; hsa:10195; hsa:25834; hsa:2683; hsa:8703; hsa:84620; hsa:4248; hsa:4247; hsa:4245; hsa:11282; hsa:23193; hsa:7841; hsa:201595; hsa:3703; hsa:1650; hsa:6184; hsa:6185; hsa:85365; hsa:56052; hsa:1798; hsa:79644; hsa:4121; hsa:57134
Cysteine and methionine metabolism	cpd:C02291; cpd:C00065; cpd:C00073; cpd:C00491; cpd:C00606; cpd:C00022; hsa:875; hsa:883; hsa:4144; hsa:10768; hsa:1786; hsa:1789; hsa:259307; hsa:58478; hsa:4357; hsa:7263; hsa:3939; hsa:3945; hsa:6611; hsa:2937; hsa:2729; hsa:2730; hsa:586; hsa:29968; hsa:26227
Alanine, aspartate and glutamate metabolism	cpd:C01042; cpd:C00049; cpd:C00152; cpd:C03794; cpd:C00158; cpd:C00122; cpd:C00022; hsa:443; hsa:339983; hsa:259307; hsa:445; hsa:435; hsa:189; hsa:2875; hsa:84706; hsa:790; hsa:7915; hsa:2746; hsa:18; hsa:8659; hsa:5471; hsa:57494
Thiamine metabolism	hsa:9054; hsa:158067; hsa:203; hsa:204; hsa:205; hsa:84284; hsa:249
Ether lipid metabolism	hsa:5051; hsa:10390; hsa:100137049; hsa:151056; hsa:283748; hsa:5320; hsa:5321; hsa:5322; hsa:81579; hsa:8398; hsa:8605; hsa:8681; hsa:23646; hsa:79888; hsa:9514
Neomycin, kanamycin and gentamicin biosynthesis	cpd:C00092; hsa:3099; hsa:3101
Phosphatidylinositol signaling system	cpd:C00416; hsa:8897; hsa:9108; hsa:113026; hsa:23236; hsa:51196; hsa:5335; hsa:5290; hsa:8503; hsa:8394; hsa:55300; hsa:5288; hsa:8760; hsa:139189; hsa:9162; hsa:5305; hsa:8396; hsa:3613; hsa:54928; hsa:3628; hsa:3632; hsa:3705; hsa:80271; hsa:23262; hsa:22908

Supplementary Table S3. ***Continued . . .***

	matched_features
Pyrimidine metabolism	cpd:C00299; cpd:C00429; cpd:C02642; cpd:C00214; cpd:C00295; cpd:C00106; hsa:6240; hsa:6241; hsa:790; hsa:7372; hsa:4831; hsa:1503; hsa:124583; hsa:957; hsa:139596; hsa:22978; hsa:51251; hsa:84618; hsa:151531; hsa:7378; hsa:1806; hsa:51733; hsa:978; hsa:79077; hsa:1841; hsa:7083; hsa:4860; hsa:1890; hsa:7298; hsa:5167; hsa:5169; hsa:318
Arginine and proline metabolism	cpd:C00581; cpd:C00300; cpd:C00134; cpd:C00315; cpd:C00148; cpd:C00077; cpd:C00022; hsa:4843; hsa:4846; hsa:113451; hsa:26; hsa:217; hsa:223; hsa:6611; hsa:112483; hsa:6303; hsa:57571; hsa:1610; hsa:112817; hsa:8659; hsa:29920; hsa:283208; hsa:5033; hsa:8974; hsa:4942; hsa:51056
Glycosaminoglycan biosynthesis - heparan sulfate / heparin	hsa:2135; hsa:2137; hsa:2131; hsa:2132
Nicotinate and nicotinamide metabolism	cpd:C00049; cpd:C05843; hsa:5167; hsa:5169; hsa:4860; hsa:64802; hsa:10135; hsa:683; hsa:952; hsa:4837; hsa:65220; hsa:22933; hsa:22978; hsa:51251; hsa:84618
Drug metabolism - other enzymes	hsa:8833; hsa:3704; hsa:9; hsa:151531; hsa:7378; hsa:1890; hsa:1806; hsa:51733; hsa:7372; hsa:7083; hsa:3614; hsa:978; hsa:1066; hsa:2990; hsa:6240; hsa:6241; hsa:4831; hsa:1571; hsa:119391; hsa:2941; hsa:2946; hsa:2947; hsa:4258
Arachidonic acid metabolism	cpd:C00219; cpd:C00157; cpd:C00584; cpd:C05951; hsa:1573; hsa:2882; hsa:493869; hsa:1571; hsa:5742; hsa:5743; hsa:100137049; hsa:151056; hsa:283748; hsa:5320; hsa:5321; hsa:5322; hsa:81579; hsa:8398; hsa:8605; hsa:8681; hsa:4056; hsa:80142; hsa:9536; hsa:8644; hsa:5730; hsa:874
Fructose and mannose metabolism	cpd:C00111; hsa:6652; hsa:3099; hsa:3101; hsa:5373; hsa:8790; hsa:2762; hsa:29925; hsa:5211; hsa:5213; hsa:7167; hsa:229; hsa:230; hsa:2203
Sphingolipid metabolism	cpd:C00065; cpd:C00346; hsa:204219; hsa:29956; hsa:91012; hsa:123099; hsa:8560; hsa:55512; hsa:55627; hsa:2531; hsa:9514; hsa:2717; hsa:129807; hsa:4758; hsa:2720; hsa:2629; hsa:7357; hsa:8877; hsa:259230
Phenylalanine metabolism	cpd:C00601; cpd:C00079; cpd:C00082; hsa:218; hsa:220; hsa:3242; hsa:259307; hsa:5053
Riboflavin metabolism	hsa:5167; hsa:5169; hsa:53; hsa:54
Butanoate metabolism	cpd:C00164; hsa:54511; hsa:3157; hsa:3158; hsa:18; hsa:35; hsa:7915; hsa:341392; hsa:54988; hsa:6296
Ascorbate and aldarate metabolism	cpd:C00167; cpd:C00818; hsa:55586; hsa:217; hsa:223
Pyruvate metabolism	cpd:C00022; cpd:C00122; hsa:5315; hsa:197257; hsa:3029; hsa:5091; hsa:3939; hsa:3945; hsa:84532; hsa:134526; hsa:217; hsa:223; hsa:1737; hsa:2271
Synthesis and degradation of ketone bodies	cpd:C00164; hsa:3157; hsa:3158; hsa:54511
Pentose and glucuronate interconversions	cpd:C00379; cpd:C00167; cpd:C00231; hsa:2990; hsa:9365; hsa:6120; hsa:9942; hsa:51084; hsa:7360; hsa:6652
Pentose phosphate pathway	cpd:C00345; cpd:C00231; hsa:2821; hsa:55276; hsa:51071; hsa:5634; hsa:22934; hsa:6120; hsa:229; hsa:230; hsa:5211; hsa:5213; hsa:2203; hsa:414328
Terpenoid backbone biosynthesis	hsa:4598; hsa:3157; hsa:3158; hsa:3422; hsa:4597; hsa:116150; hsa:79947; hsa:23590; hsa:57107; hsa:10269; hsa:23463
Galactose metabolism	cpd:C00116; hsa:2717; hsa:5211; hsa:5213; hsa:3099; hsa:3101; hsa:2720; hsa:55276; hsa:2683; hsa:2582; hsa:7360; hsa:2592; hsa:57818; hsa:92579; hsa:130589
Glycosaminoglycan biosynthesis - chondroitin sulfate / dermatan sulfate	hsa:22856; hsa:337876; hsa:55790; hsa:79586; hsa:54480; hsa:29940
Phenylalanine, tyrosine and tryptophan biosynthesis	cpd:C00079; cpd:C00082; hsa:259307; hsa:5053
Valine, leucine and isoleucine biosynthesis	cpd:C00188; cpd:C00407; cpd:C00183; hsa:586
Taurine and hypotaurine metabolism	cpd:C00606; cpd:C00245; cpd:C00519; cpd:C05122; hsa:84890
Aminoacyl-tRNA biosynthesis	cpd:C00152; cpd:C00135; cpd:C00079; cpd:C00049; cpd:C00065; cpd:C00073; cpd:C00183; cpd:C00407; cpd:C00188; cpd:C00082; cpd:C00148; hsa:10667; hsa:57038; hsa:55157; hsa:54938; hsa:55699; hsa:10352; hsa:51067; hsa:118672; hsa:51091
Propanoate metabolism	hsa:4329; hsa:84693; hsa:5095; hsa:55862; hsa:79611; hsa:84532; hsa:8802; hsa:35; hsa:26275; hsa:18; hsa:3939; hsa:3945; hsa:51
Ubiquinone and other terpenoid-quinone biosynthesis	cpd:C00082; hsa:3242; hsa:154807; hsa:79001; hsa:2677
Porphyrin and chlorophyll metabolism	cpd:C00500; cpd:C00931; cpd:C00486; hsa:326625; hsa:1355; hsa:211; hsa:2990; hsa:1356; hsa:2395; hsa:3162; hsa:3163; hsa:7390; hsa:210; hsa:3052
Sulfur metabolism	hsa:6821; hsa:54928; hsa:4357; hsa:7263; hsa:58472
Citrate cycle (TCA cycle)	cpd:C00158; cpd:C00022; cpd:C00122; hsa:4967; hsa:8802; hsa:3417; hsa:47; hsa:2271; hsa:50; hsa:5091; hsa:1737
Amino sugar and nucleotide sugar metabolism	cpd:C00167; cpd:C02336; hsa:140838; hsa:2592; hsa:2582; hsa:7360; hsa:80146; hsa:10007; hsa:5373; hsa:2762; hsa:55276; hsa:3099; hsa:3101; hsa:29925; hsa:8790; hsa:64841; hsa:51706; hsa:3073; hsa:3074; hsa:2821

Supplementary Table S3. ***Continued . . .***

	matched_features
Retinol metabolism	cpd:C00777; hsa:125; hsa:130; hsa:216; hsa:157506; hsa:5959; hsa:1543; hsa:29785; hsa:10170; hsa:10901; hsa:728635
Glycine, serine and threonine metabolism	cpd:C00065; cpd:C00581; cpd:C02291; cpd:C00213; cpd:C00188; cpd:C00300; cpd:C00022; hsa:55349; hsa:189; hsa:26227; hsa:875; hsa:29968; hsa:51268; hsa:1757; hsa:1610; hsa:211
Glycosphingolipid biosynthesis - globo and isoglobo series	hsa:53947; hsa:3073; hsa:3074; hsa:6482; hsa:6483; hsa:10690; hsa:2717
Glycosaminoglycan degradation	hsa:60495; hsa:2799; hsa:2588; hsa:6448; hsa:2720; hsa:8692; hsa:138050; hsa:3073; hsa:3074; hsa:2990
Valine, leucine and isoleucine degradation	cpd:C00164; cpd:C00183; cpd:C00407; hsa:3157; hsa:3158; hsa:54511; hsa:3712; hsa:586; hsa:10449; hsa:3032; hsa:36; hsa:35; hsa:259307; hsa:84693; hsa:5095; hsa:217; hsa:223; hsa:4329; hsa:18; hsa:26275
D-Glutamine and D-glutamate metabolism	cpd:C02237; hsa:2746
Tryptophan metabolism	cpd:C05635; cpd:C00643; cpd:C00632; cpd:C00328; hsa:3620; hsa:6999; hsa:259307; hsa:1543; hsa:15; hsa:2639; hsa:55526; hsa:8942; hsa:8564; hsa:51166; hsa:883; hsa:217; hsa:223; hsa:26
D-Arginine and D-ornithine metabolism	hsa:1610
Selenocompound metabolism	hsa:7296; hsa:22928; hsa:22929; hsa:883; hsa:51091; hsa:118672
Various types of N-glycan biosynthesis	hsa:4121; hsa:57134; hsa:2683; hsa:8703; hsa:4245; hsa:4247
Glycosylphosphatidylinositol (GPI)-anchor biosynthesis	cpd:C00350; hsa:5279; hsa:9488; hsa:23556; hsa:284098
Glyoxylate and dicarboxylate metabolism	cpd:C00158; cpd:C00065; cpd:C00022; hsa:50; hsa:112817; hsa:84693; hsa:5095; hsa:189; hsa:2653; hsa:84532
Glycosphingolipid biosynthesis - ganglio series	hsa:2720; hsa:3073; hsa:3074; hsa:6489; hsa:29906; hsa:2583; hsa:6482; hsa:6483
Phosphonate and phosphinate metabolism	hsa:10390
Caffeine metabolism	cpd:C16353; hsa:9
One carbon pool by folate	cpd:C00440; hsa:7298; hsa:4522; hsa:1719
Tyrosine metabolism	cpd:C03758; cpd:C00355; cpd:C00082; cpd:C04185; cpd:C00122; cpd:C00022; cpd:C00164; hsa:1638; hsa:218; hsa:220; hsa:125; hsa:130; hsa:3081; hsa:3242; hsa:259307
Vitamin B6 metabolism	cpd:C00534; hsa:29968
Folate biosynthesis	hsa:1719; hsa:2643; hsa:8836; hsa:249; hsa:4338; hsa:10243; hsa:55034; hsa:5053; hsa:8644
Lipoic acid metabolism	hsa:51601
Mannose type O-glycan biosynthesis	hsa:148789; hsa:84197; hsa:79147
Drug metabolism - cytochrome P450	hsa:2326; hsa:2327; hsa:1564; hsa:1565; hsa:119391; hsa:2941; hsa:2946; hsa:2947; hsa:373156; hsa:4258; hsa:125; hsa:130; hsa:218; hsa:220; hsa:1571
Biotin metabolism	hsa:3141
Fatty acid degradation	cpd:C02990; hsa:36; hsa:35; hsa:51; hsa:10449; hsa:3032; hsa:125; hsa:130; hsa:2639; hsa:217; hsa:223; hsa:2181; hsa:23305; hsa:1375
Primary bile acid biosynthesis	cpd:C00245; cpd:C00695; cpd:C05466; cpd:C05465; cpd:C01921; cpd:C05122; hsa:10858; hsa:9023; hsa:6718; hsa:3295; hsa:1582; hsa:80270
Biosynthesis of unsaturated fatty acids	cpd:C00219; cpd:C06428; cpd:C06427
Steroid biosynthesis	cpd:C05443; cpd:C01673; hsa:120227; hsa:1594; hsa:7108; hsa:4047; hsa:6307; hsa:6646
Metabolism of xenobiotics by cytochrome P450	hsa:1571; hsa:1543; hsa:119391; hsa:2941; hsa:2946; hsa:2947; hsa:373156; hsa:4258; hsa:218; hsa:220; hsa:125; hsa:130; hsa:2052; hsa:1645; hsa:1564; hsa:1565; hsa:874; hsa:29785
Fatty acid biosynthesis	cpd:C02679; cpd:C01571; hsa:84869; hsa:2181; hsa:23305
Fatty acid elongation	hsa:10449; hsa:3032; hsa:54898
Steroid hormone biosynthesis	cpd:C05476; cpd:C00762; cpd:C00951; hsa:1586; hsa:1543; hsa:1571; hsa:8644; hsa:6715; hsa:79644; hsa:1646; hsa:6718; hsa:1645; hsa:3291; hsa:3292; hsa:1588
Glycosphingolipid biosynthesis - lacto and neolacto series	hsa:10690; hsa:2526; hsa:8703; hsa:2683; hsa:2529; hsa:10402; hsa:10678; hsa:6489; hsa:84002; hsa:8707; hsa:53947